International Journal of Thermophysics, Vol. 27, No. 2, March 2006 (© 2006)
DOI: 10.1007/s10765-005-0007-0

Thermophysical Properties of Diorites along with the Prediction of Thermal Conductivity from Porosity and Density Data

I. H. Gul[1] **and A. Maqsood**[1,2]

Received March 21, 2005

The main focus of this paper involves the use of models to predict the thermophysical properties of diorites. For the prediction of thermal conductivity, an existing mixing law and empirical models have been used. Due to the porosity dependence in all the existing models, ASTM (American Society for Testing and Materials) standard methods have been applied to measure the density, porosity, and specific gravity of diorite rocks taken from the Shewa-Shahbaz Garhi volcanic complex near Mardan, Pakistan. The chemical composition of these samples has been analyzed using the X-ray florescence technique. The theoretically calculated values of specific gravity and the density of the specimen based on the chemical composition and porosity are in good agreement with those obtained from experimental measurements at ambient conditions. The thermal conductivity and thermal diffusivity of these rocks have been measured simultaneously using the transient plane source (TPS) technique at room temperature. The effective thermal conductivity calculated from various models is in agreement with the experimental data within 15%. Simple correlations between estimated density and porosity and between the effective thermal conductivity and porosity are also established.

KEY WORDS: density; diorite rocks; mixing law models; porosity; thermal conductivity; thermal diffusivity; transient plane source technique.

1. INTRODUCTION

The most important thermal properties of rocks are the thermal conductivity (λ), heat capacity (c_p), and thermal diffusivity (κ). The first two

[1] Thermal Physics Laboratory, Department of Physics, Quaid-i-Azam University, Islamabad 45320, Pakistan.
[2] To whom correspondence should be addressed. E-mail: tpl@qau.edu.pk

parameters give the capacity of a material to conduct or transmit and accumulate heat, respectively; and the last one gives an estimate of what area of the material has been affected by the heat per second. The thermal diffusivity is a function of thermal conductivity (λ), density (ρ), and specific heat capacity (c_p) at constant pressure.

The thermal conductivity of dry rocks has been shown to be a function of the density, porosity, grain size and shape, mineral composition, and the degree of cementation. The first two parameters are easily measured, and precise values may be assigned for correlation purposes. Quantification of the grain size, shape, and cementation are difficult. However, other related properties can be used to characterize these properties in developing models/correlations.

The samples studied here belong to the igneous rocks that are formed by the cooling of magma and are primary rocks (granite, diorite, basalt, dunite). They are conventionally subdivided, according to their silica content [1, 2], into the granite group ($SiO_2 > 65\%$), diorite ($SiO_2 = 65$ to 52%), basalt ($SiO_2 = 52 - 40\%$), and dunite ($SiO_2 < 40\%$). The samples studied in this paper belong to the diorite group.

The thermal transport properties of 13 diorite samples taken from the Shewa-Shahbaz Ghari volcanic complex have been measured using the transient plane source (TPS) technique. The Shewa-Shahbaz Ghari volcanic complex is located about 60 km south of the Indus River and is an isolated triangular outcrop exposed between Shewa-Shahbaz Ghari and the Machai, which represent corners of the complex. It covers an area of about 85 km^2 and is emplaced into a meta-sedimentary sequence known as the Swabi-Chamla group.

As reported earlier [3] the National Centre of Excellence in Geology and Mineral Testing Laboratory and the Serhad Development Authority, Peshawar (Pakistan) have been involved in petrological investigations and the study of the physical properties of these rocks from an application point of view. Our research group undertook a study of the thermophysical properties with the availability of the well-developed TPS technique and other physical methods of measurements. The variations of thermal conductivity, thermal diffusivity, and volumetric heat capacity in the temperature range from 253 to 333 K have already been reported [3]. All the samples under study were characterized by chemical composition, density, porosity, and specific gravity at ambient conditions.

In this study, simple models to predict the thermal conductivity of diorites based on the porosity and thermal conductivity data of the mineral contents and saturant have been established using mixing law and empirical models [4, 5] at ambient conditions. The predicted values of the thermal conductivity have been compared with the experimental

measurements. Simple correlations between the estimated density and porosity and between the effective thermal conductivity and porosity are also established.

2. MODELS FOR ESTIMATION OF THERMAL CONDUCTIVITY

Precise measurements of thermal conductivities of rocks are difficult to make and are very time-consuming. To make laboratory measurements on all types of rock of interest and under all environmental conditions of temperature, pressure, and fluid saturation would be prohibitive in terms of time and expense. There have been many attempts [4, 6–11] to develop a simple physical model to explain the measured thermal conductivities of porous rocks filled with fluids ranging in conductivity from that of air to that of water. Three basic types of models for the thermal conductivity of multicomponent system have been used in the past. The first type involves the application of mixing laws for porous mineral aggregates containing various fluids. Since these models do not take into account the structural characteristics of rocks, they are of limited applicability. A second type is the empirical model in which more easily measured physical properties are related to thermal conductivity through the application of regression analysis to laboratory data. This method also has its shortcomings in that the resulting model may be applicable only to the particular suite of rocks being investigated. For example in two separate papers, Sugawara and Yoshizawa [7, 8] have chosen different exponents for essentially identical sets of experiments on similar rocks. The third type is a theoretical model based on the mechanism of heat transfer applicable to simplified geometries of the rock/fluid system. In the literature, efforts in this direction have been made by many authors [9, 12–18]. The proposed models have limited applicability and cannot be used for all types of systems, especially when the difference in the thermal conductivities of the constituent phases is very large. A general expression to predict the effective thermal conductivity is still lacking. A short description of the models used for the estimation of thermal conductivity of diorites is given below.

2.1. Mixing Law Models

If we assume that minerals with thermal conductivities λ_i and volume concentration V_i are arranged in parallel in a nonporous rock, then the thermal conductivity λ_s of the solid rock will be

$$\lambda_s = \frac{\Sigma \lambda_i V_i}{\Sigma V_i}. \tag{1}$$

Mixing law models combine values of the thermal conductivities of the rock solids (λ_s) with the thermal conductivity of the fluids (λ_f) on the basis of porosity (ϕ). The porosity weighted arithmetic mean would be the equivalent of parallel arrangement of the components relative to the direction of heat flow;

$$\lambda_e = \lambda_f \phi + \lambda_s (1 - \phi), \tag{2}$$

where λ_s and λ_f are the thermal conductivities of the rock solids and the fluid, respectively. This form gives the largest values of thermal conductivity of the rock/fluid system (λ_e) of all the mixing law models. The harmonic mean model would imply a series arrangement of the components,

$$\lambda_e = \left[\frac{\phi}{\lambda_f} + \frac{1 - \phi}{\lambda_s} \right]^{-1}. \tag{3}$$

This model gives the smallest values of λ_e.

A modification of the weighted arithmetic mean or parallel model, Eq. (2), was used by Sugawara and Yoshizawa [8] to obtain good agreement between their experimental and estimated thermal conductivities of two-phase, fluid-saturated rocks. Their model is given as

$$\lambda_e = (1 - A)\lambda_s + A\lambda_f, \tag{4}$$

where

$$A = \left\lfloor 2^n \left(2^n - 1\right)^{-1} \right\rfloor \left[1 - (1 + \phi)^{-n}\right],$$

and $n > 0$ is an empirical exponent dependent on the porosity, shape, orientation, and emissivity inside the pores.

The geometric mean model of Woodside and Messmer [19] is expressed as

$$\lambda_e = (\lambda_f)^{\phi} \lambda_s^{(1-\phi)}. \tag{5}$$

The dispersive or extended Maxwell model has a thermal conductivity [4] given by

$$\lambda_e = \lambda_s \left[\frac{\left(\frac{2\lambda_s}{\lambda_f} + 1\right) - 2\phi\left(\frac{\lambda_s}{\lambda_f} - 1\right)}{\left(\frac{2\lambda_s}{\lambda_f} + 1\right) + \phi\left(\frac{\lambda_s}{\lambda_f} - 1\right)} \right]. \tag{6}$$

The first two models, Eqs. (2) and (3), have a firm physical basis, but are essentially special cases, which are unrealistic in most practical situations. The weighted geometric mean model, Eq. (5), has no physical basis,

but it is easier to use than Eq. (6) and gives similar results over the limited range of heat flow work; some authors prefer to use it.

The Maxwell model [20], which is the direct analog of the electrical case and has a good physical basis, gives quite reliable results when the porosity (ϕ) of one of the two components does not exceed about 0.25 and the conductivity ratio ($r = \lambda_s/\lambda_f$) does not exceed 10. Beck [4], using an empirical approach, extended the useful range of porosity ($\phi > 0.3$) and $r > 300$.

2.2. Empirical Correlations

The effects of a number of physical properties on thermal conductivities of several dry sandstone samples have been investigated [21, 22] and the existence of several correlations between thermal conductivity, density, and porosity are reported. For example,

$$\lambda_e \propto \rho^4, \tag{7}$$

where λ_e is the thermal conductivity in $W \cdot m^{-1} \cdot K^{-1}$ and ρ is the bulk density. The bulk density is also correlated with the porosity as

$$\rho \propto (1 - \phi), \tag{8}$$

and by substituting Eq. (8) into (7), one obtains

$$\lambda_e \propto (1 - \phi)^4. \tag{9}$$

The proportionality constants may vary according to the suite of rocks. Extrapolations of empirical models to suites of rocks other than those used in developing the correlation equations may not be reliable.

3. MEASURED PROPERTIES

3.1. Density-Related Properties

Density-related properties of rocks include specific gravity, density, and porosity. These parameters have one thing in common, the fact that they have no connection with any external factor and so are not mechanical. They must, however, be considered first before any other properties of rocks can be studied.

In our experimental work, the definitions of the American Society for Testing and Materials Standards (ASTM) [23] have been followed. The density, porosity, and specific gravity of the samples were measured by using ASTM standard methods, and details are already given [24].

3.2. Thermal Transport Properties

The TPS technique, also known as the Gustafsson probe [25], was used to perform simultaneous measurements of thermal conductivity, thermal diffusivity, and heat capacity per unit volume of the diorites. This technique is based on three-dimensional heat flow inside the sample, which can be regarded as an infinite medium, if the time of the transient recording is ended before the thermal wave reaches the sample boundaries. The TPS method uses a resistive element both as a heat source and a temperature sensor. For data collection the TPS element (20 mm diameter) is sandwiched between two specimen halves in a bridge circuit [25]. When a sufficiently large amount of direct current is passed through the TPS element, its temperature changes, which causes its resistance to change and consequently there is a voltage drop across the TPS element. By recording this voltage drop for a particular time interval, detailed information about the thermal conductivity and thermal diffusivity of the test specimen is obtained. The heat capacity per unit volume is then calculated from $\rho c_p = \lambda/\kappa$. For further details, see Gustafsson [26].

The entire samples were taken from the Shewa-Shahbaz Garhi volcanic complex near Mardan, Pakistan. These samples were then cut into rectangular shapes. Each sample consisted of two identical rectangular slabs of approximately 0.045 m $\times$ 0.045 m $\times$ 0.025 m. The chemical compositions were analyzed using the X-ray fluorescence technique and are given in Table I. The surfaces of these samples were polished to provide good thermal contact with the TPS element and to minimize thermal contact resistance.

Table I. Chemical Composition of Diorite Samples (in Mass%).

Sample	SiO_2	TiO_2	Al_2O_3	Fe_2O_3	FeO	MnO	MgO	CaO	Na_2O	K_2O	P_2O_5
SSG-D1	55.25	0.08	24.28	1.13	1.02	0.41	0.01	0.74	13.83	4.71	0.02
SSG-D2	57.03	0.27	23.11	0.87	1.40	0.10	0.25	1.21	10.13	5.55	0.04
SSG-D3	58.30	0.11	21.34	0.67	1.07	0.08	0.06	0.68	11.16	6.52	0.02
SSG-D4	58.63	0.72	20.68	1.19	1.91	0.20	0.73	2.26	7.92	5.64	0.12
SSG-D5	58.77	0.94	19.08	1.82	2.91	0.21	1.21	2.86	6.88	5.16	0.25
SSG-D6	58.77	1.53	17.28	2.98	3.28	0.17	1.78	4.06	5.20	4.54	0.42
SSG-D7	58.87	0.16	21.92	1.12	1.80	0.13	0.08	0.67	10.28	4.95	0.01
SSG-D8	60.83	0.84	18.6	1.87	2.06	0.17	0.45	2.10	5.50	7.52	0.05
SSG-D9	61.63	0.58	19.47	1.03	1.64	0.16	0.28	1.25	7.99	5.93	0.04
SSG-D10	61.77	0.83	18.24	1.72	1.92	0.15	0.43	1.95	5.51	7.43	0.07
SSG-D11	61.87	0.52	19.33	1.21	1.92	0.12	0.23	1.45	7.27	6.04	0.04
SSG-D12	62.17	0.46	18.90	1.16	1.86	0.10	0.23	1.79	7.58	5.73	0.03
SSG-D13	63.93	0.46	18.63	1.38	1.52	0.11	0.35	1.23	7.09	5.38	0.12

Measurements of thermophysical properties were carried out with air as the saturant in the pore spaces. For this purpose, the samples were dried at $105 \pm 2^{\circ}C$ in a furnace (Heraeus laboratory furnace M110) for 24 h. After drying, the samples were cooled at room temperature for 30 minutes and then placed in a closed desiccator (to avoid any moisture interference). For every sample, four experiments were carried out; as described earlier [25]. The thermal conductivity and thermal diffusivity of 13 samples were measured at room temperature and atmospheric pressure. The thermal conductivity and thermal diffusivity data include uncertainties of 5 and 7%, respectively.

4. RESULTS AND DISCUSSION

4.1. Density-Related Properties

Table II gives the measured values of specific gravity (a_0), porosity (ϕ), and density (ρ). The specific gravity of the minerals depends on the chemical composition and structure. The specific gravity of all these samples lies between 2.554 and 2.838. This is explained by the fact that the specific gravity of slightly porous rocks depends on the extent of their mineral composition. In these samples SiO_2 lies between 55 and 64% and the specific gravity of SiO_2 is 2.65. Also, the specific gravity of igneous rocks ranges from 2.17 to 3.74. Thus, these reported measurements are in good agreement with the earlier studies [2]. As noted earlier, the specific gravity of a rock is wholly dependent on the specific gravity of minerals forming it. This parameter can be predicted by using the Felsic-mafic index F [27] that provides a better correlation curve than the silica content when attempts are made to correlate specific gravity and chemical composition. However, the correlation becomes less useful when the rock is more felsic than quartz monzonite. The useful curve of Young and Olhoeft [27] is

$$\text{specific gravity } (a_{\text{est}}) = 2.643 + 0.444e^{-F/4},$$

where

$$F = \frac{SiO_2 + Na_2O + K_2O}{FeO + Fe_2O_3 + CaO + MgO}. \tag{10}$$

Using this relation and the data of Table I, a_{est} of all the samples was calculated and is tabulated in Table II. There is good agreement between the observed and calculated specific gravity parameters. Table II also shows the porosity and density of the diorite samples. The porosity of these samples varies from 0.162 to 0.490 vol%. This variation in porosity depends on the composition of the samples and the shape and size of

Table II. Measured Specific Gravity (a_0), Estimated Specific Gravity (a_{est}), Measured Porosity (ϕ) and Density (ρ), and Estimated Density (ρ_{est}) of the Specimens at Normal Temperature and Pressure

S. No.	$a_0 \pm 0.003$	a_{est}	ϕ(vol%)	ρ (10^3 kg $\cdot m^{-3}$) ± 0.002	ρ_{est} (10^3 kg $\cdot m^{-3}$)
SSG-D1	2.624	2.644	0.335	2.615	2.641
SSG-D2	2.599	2.646	0.167	2.594	2.646
SSG-D3	2.603	2.643	0.162	2.599	2.646
SSG-D4	2.608	2.666	0.490	2.595	2.637
SSG-D5	2.718	2.702	0.353	2.708	2.641
SSG-D6	2.838	2.751	0.397	2.827	2.639
SSG-D7	2.589	2.646	0.234	2.583	2.644
SSG-D8	2.723	2.669	0.469	2.411	2.638
SSG-D9	2.627	2.648	0.206	2.622	2.645
SSG-D10	2.621	2.663	0.347	2.612	2.641
SSG-D11	2.624	2.652	0.424	2.613	2.638
SSG-D12	2.554	2.653	0.413	2.544	2.639
SSG-D13	2.706	2.649	0.358	2.697	2.641

the grains of which they are composed and on the degree of their sorting, cementation, and packing.

The density of the samples lies between (2.411 and 2.827) $\times 10^3$ kg $\cdot$ m^{-3}. These values are again in agreement with the reported data. It was possible to establish a correlation between bulk density and fractional porosity for the rock samples as

$$\rho_{est} = 2.65 \times 10^3 (1 - \phi), \tag{11}$$

where ρ_{est} is the bulk density in kg $\cdot$ m^{-3} and the density of SiO_2 is 2.56×10^3 kg $\cdot$ m^{-3}.

As is evident from Table II, there exists excellent agreement between the experimental and estimated bulk densities and specific gravities.

4.2. Thermal Diffusivity and Thermal Conductivity at Ambient Conditions

In Fig. 1, the thermal diffusivity is plotted as a function of the thermal conductivity at ambient temperature. A linear regression yields a slope of $1/\rho c_p = 1/2.33 \times 10^6 \mathrm{J} \cdot \mathrm{m}^{-3} \cdot K^{-1}$; this agrees with Beck's [28] result $\rho c_p = 2.3 \times 10^6$ J $\cdot$ m^{-3} $\cdot$ K^{-1} $\pm 20\%$.

The remainder of this discussion involves the calculation of the thermal conductivity using the above models. As shown in Table III, λ_{exp} lies between 1.422 and 1.688 W $\cdot$ m^{-1} $\cdot$ K^{-1}at room temperature, and normal

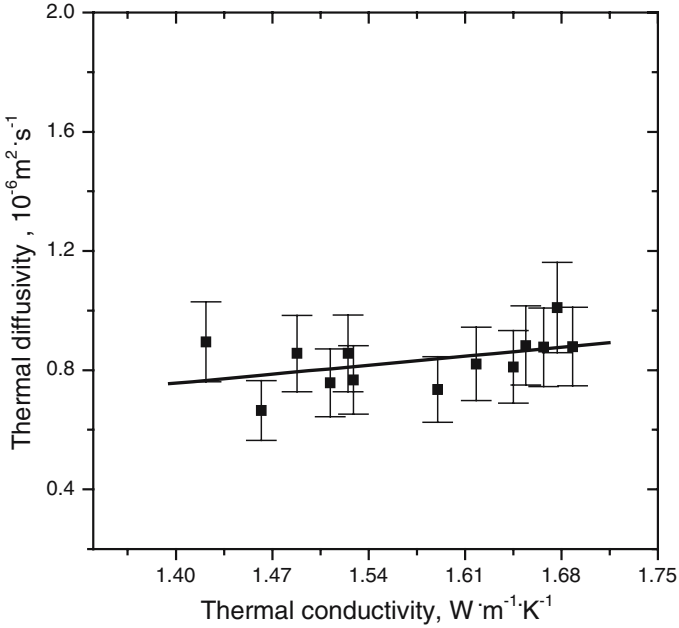

Fig. 1. Variation of thermal diffusivity as a function of thermal conductivity along with linear fit (solid line).

pressure. The thermal conductivity of the solid phase, λ_s, was assumed to be 1.5 $W \cdot m^{-1} \cdot K^{-1}$, corresponding to biotite [30, 31] and $\lambda_f = \lambda_{air} = 0.026$ $W \cdot m^{-1} \cdot K^{-1}$ [32] for the calculation of the effective thermal conductivity (λ_e) of the samples.

All of the samples have more or less similar composition (Table II), with a porosity ranging from 0.162 to 0.490 vol%. Using the values of λ_s, λ_f, and ϕ, the effective thermal conductivities corresponding to the mixing law models, Eqs. (2) and (6), and the empirical relation, Eq. (9), were calculated and are compared in Table III and Fig. 2.

The experimentally measured thermal conductivity values are higher than the effective thermal conductivity values, for all the models for $\phi <$ 0.35 vol%, although the average deviation is within 10%. For $\phi > 0.35$ vol%, the effective values are higher compared to the experimentally measured values and the difference is within 8%.

For low porosities ($\phi < 1$ vol%) two models have been proposed by Walsh and Decker [29]:

(a) for isolated, more or less, isometric pores, a "minimum" value,

Table III. Experimental (λ) and Effective (λ_e) Thermal Conductivities, Calculated According to Different Relations, are Given for Diorites along with the Percentage Deviation (% Dev.) at Normal Temperature and Pressure (Values of Thermal Conductivity are in $W \cdot m^{-1} \cdot K^{-1}$.)

		$\lambda_e = \lambda_f \phi + \lambda_s (1-\phi)$		$\lambda_e = (\lambda_f)^{\phi} + \lambda_s^{(1-\phi)}$		$\lambda_e = \lambda_s - A(\lambda_s - \lambda_f)$		Maxwell model		$\lambda_e = 1.5(1-\phi)^4$		Walsh and Decker [29] Eq. (13)	
Specimen	$\lambda_{exp.}$	λ_e	% dev.	λ_e	% dev.	λ_e	% dev.	λ_e	% dev.	λ_e	% dev.	% dev.	λ_e
SSG-D1	1.512	1.495	1.12	1.480	2.12	1.490	1.46	1.493	1.26	1.480	2.12	1.411	6.68
SSG-D2	1.488	1.498	0.67	1.490	0.13	1.495	0.47	1.496	0.56	1.490	2.90	1.454	2.55
SSG-D3	1.525	1.498	1.77	1.490	2.30	1.495	1.97	1.496	1.87	1.490	2.30	1.455	4.52
SSG-D4	1.462	1.493	2.12	1.470	0.55	1.486	3.94	1.489	1.85	1.471	0.62	1.373	5.42
SSG-D5	1.422	1.495	5.13	1.479	4.01	1.490	4.78	1.492	4.94	1.479	4.01	1.406	1.13
SSG-D6	1.590	1.494	6.04	1.476	7.17	1.488	4.62	1.491	6.21	1.476	7.17	1.395	12.26
SSG-D7	1.529	1.497	2.09	1.487	2.75	1.493	2.35	1.495	2.22	1.486	2.81	1.437	6.22
SSG-D8	1.618	1.493	7.73	1.472	9.02	1.486	8.16	1.490	7.91	1.472	9.02	1.378	14.83
SSG-D9	1.677	1.497	10.73	1.489	11.21	1.494	10.91	1.495	10.91	1.448	11.27	1.444	13.89
SSG-D10	1.654	1.495	9.61	1.479	10.58	1.490	9.92	1.492	9.79	1.479	10.58	1.408	14.87
SSG-D11	1.645	1.494	9.18	1.472	10.52	1.488	9.54	1.491	9.36	1.475	10.33	1.389	15.38
SSG-D12	1.669	1.494	10.49	1.475	11.62	1.488	10.84	1.491	10.67	1.475	11.62	1.392	16.60
SSG-D13	1.688	1.495	11.43	1.478	12.44	1.490	11.76	1.492	11.61	1.479	12.38	1.405	16.77

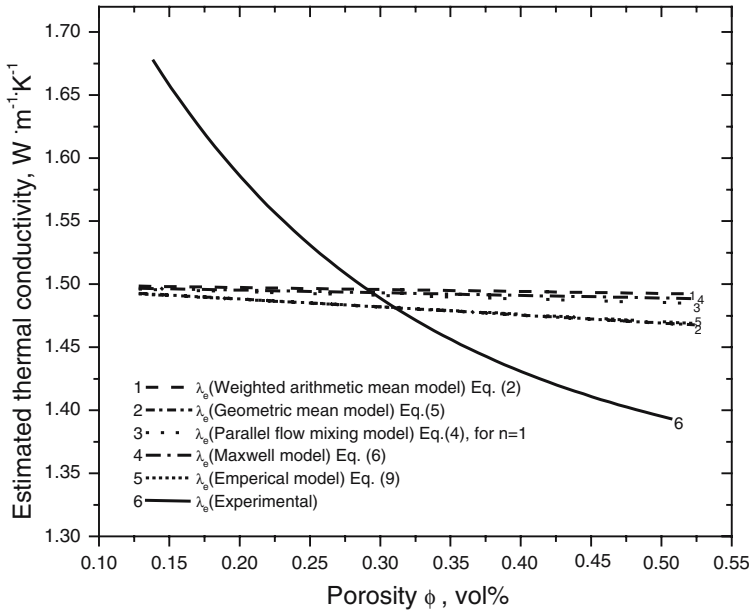

Fig. 2. Comparison of measured and predicted thermal conductivities of diorite samples as a function of porosity (vol%).

$$\lambda_e = \lambda_s \left\{ \frac{1 - 3\phi \left[1 - \left(\frac{\lambda_f}{\lambda_s} \right) \right]}{2 + \phi + \left(\frac{\lambda_s}{\lambda_f} \right)} \right\}, \tag{12}$$

and

(b) for interconnected, rock-type pores, a "maximum" value,

$$\lambda_e = \frac{\lambda_s \lambda_f (3 + \phi)}{\phi \lambda_s + 3\lambda_f}, \tag{13}$$

Using Eq. (13), the effective thermal conductivity was calculated and λ_e appeared to be much lower compared to all the other models (Table III). This is the shortcoming of these models, and they are often suitable for a given suite of samples. Similarly, the modified weighted arithmetic mean model proposed by Sugawara and Yoshizawa, Eq. (5), gave $\lambda_e$values for $n = 1$, which agreed with experimental data within experimental error.

In sedimentary rocks the primary porosity is subjected to digenitic changes and further to processes like fracturing which may lead to secondary porosity. Therefore, pores can be present in different forms and

configurations, to which all the above models could contribute, depending upon the grain type and size of the rock in question. All models as well as the correlations between λ_e and ϕ appear to be suitable within 10%. For the values of porosities $\phi < 0.35$ vol%, all the models used here gave lower values compared to experimental results, and for $\phi > 0.35$ vol%, experimental results are lower than the calculated values. It is to be noted that the experimental as well as the calculated values of λ_e using different models decreases with an increase of the porosity. This observation is in agreement with others [8, 19, 33].

5. CONCLUSIONS

The diorite samples have been characterized by chemical composition, porosity, and density. ASTM standard methods have been applied to study the density-related properties. Simple correlations between the chemical compositions and specific gravity, density, and porosity are established. The chemical composition of these samples has been analyzed using the X-ray florescence technique. The theoretically calculated values of specific gravity and density of the specimen based on the chemical composition and porosity were in good agreement with those obtained from experimental observations. The thermal transport experiments were performed at room temperature and normal pressure with air as the fluid in the pore spaces, using the Gustafsson probe. The thermal diffusivity varies linearly with thermal conductivity. To predict the thermal conductivity of diorite samples, the existing mixing law and empirical models have been used. Empirical models are often used as an alternative, and they are generally satisfactory for a given suite of rocks. In this study, it is noted that experimental and calculated thermal conductivity values are in agreement within 10% on the average as shown in Table III.

ACKNOWLEDGMENTS

The authors are grateful to the Higher Education Commission, Pakistan and Quaid-i-Azam University for supporting the present work financially. Dr. Anis-ur-Rehman is acknowledged for useful discussion.

REFERENCES

1. V. Rzhevsky and G. Novik, *The Physics of Rocks* (Mir, Moscow, 1971).
2. Y. S. Touloukian, W. R. Judd, and R. F. Roy, *Physical Properties of Rocks and Minerals* (McGraw-Hill, New York, 1981).
3. A. Maqsood, I. H. Gul, and M. A. Rehman, *Int. J. Thermophys.* **25**:1943 (2004)

4. A. E. Beck, *Geophysics* **41**:133 (1976).
5. U. Scharli and L. Rybach, *Technophys.* **103**:307 (1984).
6. W. D. Kingery, *J. Am. Ceram. Soc.* **42**:617 (1959).
7. A. Sugawara and Y. Yoshizawa, *Australian J. Phys*. **14**:468 (1961).
8. A. Sugawara and Y. Yoshizawa, *J. Appl. Phys*. **33**:3135 (1962).
9. R. W. Zimmerman, *J. Pet. Sci. Eng*. **3**:219 (1989).
10. A. Bouguerra, *J. Phys. D: Appl. Phys.* **32**:1407 (1999).
11. K. J. Singh, R. Singh, and D. R. Chaudhary, *J. Phys. D: Appl. Phys*. **31**:163 (1998).
12. K. Lichtnecker, *Z. Phys.* **27**:115 (1926).
13. A. A. Babanov, *Sov. Phys. Tech. Phys.* **2**:476 (1957).
14. A. D. Brailsford and K. G. Major, *Br. J. Appl. Phys.* **15**:313 (1964).
15. J. Huetz, *Progress in Heat and Mass Transfer* (Pergamon, Oxford, 1970).
16. V. Kummar and D. R. Chaudhary, *Ind. J. Pure Appl. Phys*. **18**:984 (1980).
17. R. N. Pande, V. Kumar, and D. R. Chaudhary, *Pramana* **22**:63 (1984).
18. K. Misra, A. K. Shrotriya, R. Singh, and D. R. Chaudhary, *J. Phys. D: Appl. Phys*. **27**:732 (1994).
19. W. Woodside and J. H. Messmer, *J. Appl. Phys*. **32**:1688 (1961).
20. J. C. Maxwell, *A Treatise of Electricity and Magnetism*, Vol 1, 3rd Ed. (Clarendon, Oxford, 1904).
21. J. Anand, W. H. Somerton, and E. Gomaa, *Soc. Petrol. Eng. J.* **13**:267 (1973).
22. W. H. Somerton, *Thermal Properties and Temperature Related Behaviour of Rock/Fluid Systems* (Elsevier, New York, 1992).
23. *Annual Book of ASTM Standards*, C20 (ASTM International, West Conshohocken, Pennsylvania, 1973).
24. A. Maqsood, M. A. Rehman, and I. H. Gul, *J. Chem. Eng. Data* **48**:1310 (2003).
25. G. Shabbir, M. Maqsood, A. Maqsood, I. Haq, N. Amin, and S. E. Gustafsson, *J. Phys. D: Appl. Phys.* **26**:1576 (1993).
26. S. E. Gustafsson, *Rev. Sci. Instrum.* **62**:797 (1991).
27. E. J. Young and G. R. Olhoeft, *U.S. Geological Survey Open File* (1976).
28. A. E. Beck, in *Handbook of Terrestrial Heat – Flow Density Determination*, R. Haenel, L. Rybach, and L. Stegena, eds. (Kluwer Academic Publisher, Dordrecht, 1988).
29. B. J. Walsh and E. R. Decker, *J. Geophys. Res.* **71**:3053 (1966).
30. V. Cermak and L. Rybach, *Thermal Properties: Thermal conductivity and Specific Heat of Minerals and Rocks* (Springer Verlag, Berlin, Heidelberg, New York, 1982).
31. E. Huenges and G. Will, *Permeability, Bulk Modulus and Complex Resistivity in Crystalline Rocks, in Fluid Movements – Element Transport and the Composition of the Deep Crust. NATO ASI Series* (Kluwer Academic Publisher, Dordrecht, 1989).
32. K. Horai, *J. Geophys. Res.* **76**:617 (1971).
33. A. Maqsood, K. Kamran, and I. H. Gul, *J. Phys. D: Appl. Phys.* **37**:3396 (2004).